

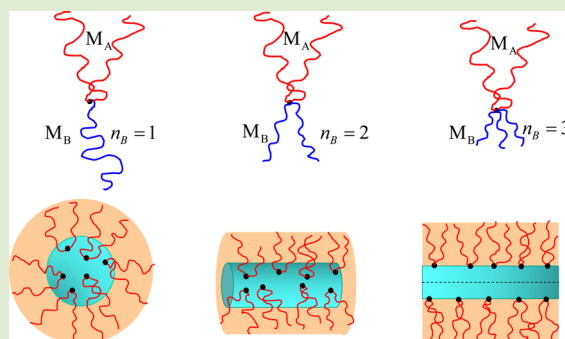
# Effect of Block Copolymer Architecture on Morphology of Self-Assembled Aggregates in Solution

E. B. Zhulina<sup>†</sup> and O. V. Borisov<sup>\*,†,‡</sup>

<sup>†</sup>Institute of Macromolecular Compounds of the Russian Academy of Sciences, St. Petersburg, Russia

<sup>‡</sup>IPREM UMR 5254 CNRS UPPA, Pau, France

**ABSTRACT:** We predict how equilibrium morphology of self-assembled aggregates in dilute solution could be tuned by replacing a linear AB diblock copolymer by a heteroarm star-like or cyclic block copolymer. We demonstrate that in selective solvent AB miktoarm stars or diblock copolymers with cyclic associating block may give rise to cylindrical assemblies or vesicles, while linear diblock copolymers with same composition form only spherical micelles. The theoretical predictions are in line with experimental observations.



Self-assembly in solutions of linear block copolymers has been very much in the focus of theoretical and experimental research in the past decade.<sup>1–6</sup> This interest was primarily motivated by applications of polymer self-organization in fabrication of functional materials and nanoscale devices. Among the examples are vector systems for controlled delivery and release of biologically active molecules, nanocatalytic systems, molecular templates, etc.

A systematic theoretical relationship between the composition of the AB block copolymer and the equilibrium shape of aggregates forming in dilute and semidilute solutions has been first established for nonionic macromolecules.<sup>7,8</sup> It was predicted and confirmed experimentally that an increase in length of insoluble block changes morphology from a spherical micelle toward cylindrical aggregates and vesicles (polymerosomes). The theory<sup>8</sup> demonstrated that in dilute solutions cylindrical micelles and vesicles are thermodynamically stable only when the characteristic dimensions of insoluble (core) domains are comparable to or exceed the dimensions of solvated (coronal) domains. Similar regularities have been established for amphiphilic ionic/hydrophobic AB block copolymers in aqueous solutions.<sup>9–11</sup>

Branching could strongly effect the self-assembly of block copolymers. Self-organization of star-like macromolecules in melts is rather well comprehended.<sup>12–15</sup> The understanding of self-assembly of miktoarm star polymers in solutions is less evolved. The relevant studies focused mostly on the effect of branching on the parameters of micelles with specific morphology, e.g., spherical<sup>16–19</sup> or lamellar.<sup>20</sup> In this letter we examine how the copolymer branching affects the equilibrium morphology of self-assembling aggregates. Recent experimental studies<sup>21–25</sup> demonstrated that a star-like block copolymer with a sufficiently large number of long soluble arms and/or with a small number of short insoluble arms gives rise to

stable unimolecular spherical micelles. Here, we focus on the opposite case of multichain aggregates and establish how the stability range of classical morphologies (sphere, cylinder, lamella) depends on the molecular parameters of the AB miktoarm copolymer. We then apply the developed model to a cyclic diblock copolymer and compare our theoretical predictions with the experimental findings.<sup>26–29</sup>

We consider a dilute solution of miktoarm stars in selective solvent. Each molecule consists of  $n_B \geq 1$  insoluble blocks, each comprising  $N_B \gg 1$  monomer units, and of  $n_A \geq 1$  soluble blocks, each of  $N_A \gg 1$  monomer units (see Figure 1a). We assume, for simplicity, that both components have the same monomer unit size,  $a$ , and are equally flexible (the length of the Kuhn segment is on the order of  $a$ ). Total amounts of monomer units A and B in the macromolecule are  $M_A = n_A N_A$

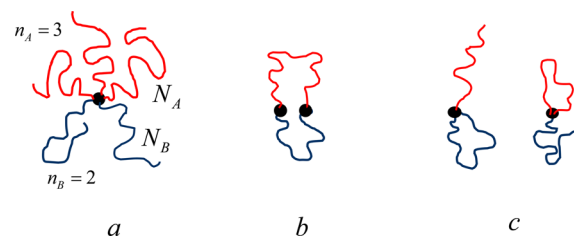


**Figure 1.** Miktoarm star-like copolymer:  $n_A$ ,  $N_A$  and  $n_B$ ,  $N_B$  are the number of soluble and insoluble arms and the number of monomer units per arm, respectively (a), cyclic block copolymer (b), and linear block copolymer with cyclic block B or A (c).

**Received:** January 28, 2013

**Accepted:** March 12, 2013

**Published:** March 21, 2013

and  $M_B = n_B N_B$ , respectively. The case  $n_A = n_B = 1$  corresponds to a linear diblock copolymer.

Association of insoluble domains B leads to formation of multimolecular aggregates with radius of the core

$$R_i = a^3 \frac{i N_B n_B}{\varphi s} = a^3 \frac{i M_B}{\varphi s} \quad (1)$$

where  $s$  is area per macromolecule at the core/corona interface, and  $\varphi$  is volume fraction of monomer units B in the core. Below we assign  $i = 1$  to lamella (or vesicle),  $i = 2$  to cylindrical aggregate, and  $i = 3$  to spherical micelle (see Figure 2) and set  $\varphi \simeq 1$ .

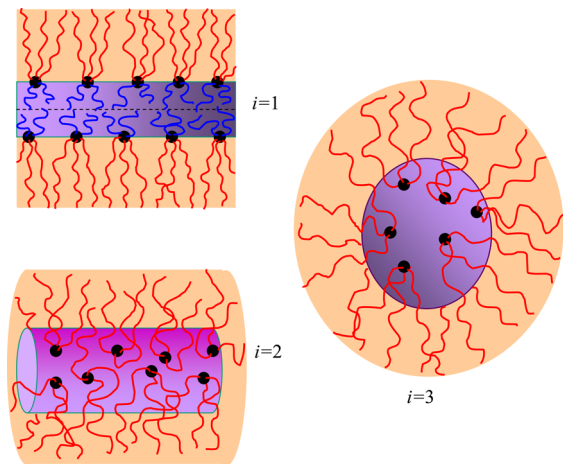


**Figure 2.** Schematics of generic morphologies of self-assembled aggregates of miktoarm star copolymers: lamellae or vesicles (top left), cylindrical micelles (bottom left), spherical micelles (right).

The free energy (per star-like molecule) in aggregate of morphology  $i$  is given by

$$F_i = F_{i,\text{corona}} + F_{i,\text{core}} + F_{\text{surface}} \quad (2)$$

In the narrow interface approximation, the corona of the micelle is envisioned as a polymer brush with grafting area  $s/n_A$  per soluble block A, and

$$F_{i,\text{corona}} = n_A F_{i,\text{brush}}(s/n_A) \quad (3)$$

where  $F_{i,\text{brush}}(s/n_A)$  is the free energy per block A. The functional form of  $F_{i,\text{brush}}$  is governed by the nature of the soluble blocks (e.g., presence/absence of ionizable groups), solvent quality, etc.<sup>3</sup> The morphology-dependent core contribution (per molecule) comprises the free energy of elastic stretching of blocks B in the micellar core

$$\frac{F_{i,\text{core}}}{k_B T} \simeq n_B \frac{b_i R_i^2}{a^2 N_B} = n_B^3 \frac{i^2 b_i a^4 N_B}{s^2} = n_B^2 \frac{i^2 b_i a^4 M_B}{s^2} \quad (4)$$

with numerical coefficients<sup>30</sup>  $b_1 = \pi^2/8$ ,  $b_2 = \pi^2/16$ , and  $b_3 = 3\pi^2/80$ . Finally, the surface free energy

$$\frac{F_{i,\text{surface}}}{k_B T} = \gamma s / a^2 \quad (5)$$

is controlled by excess free energy  $\gamma$  at the core/corona interface (measured in units of  $k_B T$  per area  $a^2$ ) and by area  $s$  per molecule. Minimization of  $F_i$  with respect to surface area  $s$  provides equilibrium parameters of aggregates with morphology

$i$ . The regions of thermodynamic stability of the aggregates with morphologies  $i = 1, 2, 3$  are specified by minimal values of  $F_i$ .

Morphological transformations of aggregates are expected when the aggregates have crew-cut shape,<sup>8,9</sup> that is, when the corona thickness  $H_i$  is smaller than (or comparable to) the radius  $R_i$  of the insoluble core. The corona of an aggregate with  $H_i/R_i \ll 1$  can be envisioned as a weakly curved polymer brush with the free energy per molecule  $F_{i,\text{corona}} = F_{1,\text{corona}} - \Delta F_{i,\text{corona}}$  where  $F_{1,\text{corona}}$  corresponds to a planar brush ( $i = 1$ ), and the linear in curvature correction term is given by

$$\Delta F_{i,\text{corona}} \simeq F_{1,\text{corona}} \times (i-1) \frac{H_{1,\text{corona}}}{R_i} \ll F_{i,\text{corona}} \quad (6)$$

The value of the numerical coefficient omitted in eq 6 as well as the power law expressions for  $F_{1,\text{corona}}$  and  $H_{1,\text{corona}}$  depend on the nature of the coronal blocks (nonionic or ionic) and on the environmental conditions (solvent quality, ionic strength, pH, etc.)<sup>31</sup>

For block copolymer with long blocks ( $N_A, N_B \gg 1$ ), approximate power law dependencies for binodals, separating regions in the phase diagram corresponding to stable aggregates with morphologies  $i$  and  $i+1$ , could be obtained by balancing the free energy gain due to convex corona bending with the free energy loss due to extra elastic stretching of core blocks,  $-\Delta F_{i,\text{corona}} + F_{i,\text{core}} = -\Delta F_{i+1,\text{corona}} + F_{i+1,\text{core}}$ . By omitting the numerical coefficients, using eqs 6 and 4, and applying eq 1, we obtain the equation for binodal lines at which morphologies  $i$  and  $i+1$  coexist in equilibrium

$$(n_B^2 N_B)^{i \rightarrow i+1} \simeq \sqrt{\frac{s^3 F_{1,\text{corona}}(s) H_{1,\text{corona}}(s)}{i(i+1)[b_{i+1}(i+1)^2 - b_i^2] a^7 k_B T}} \quad (7)$$

with  $s$  specified below. As follows from eq 7, the values of  $n_B^2 N_B$  corresponding to cylinder-to-sphere ( $c-s$ ,  $i = 2$ ) or to lamella-to-cylinder ( $l-c$ ,  $i = 1$ ) transitions differ only by the numerical coefficient,  $(n_B^2 N_B)^{(c-s)/(l-c)} / (n_B^2 N_B)^{(l-c)} = (10/21)^{1/2}$ . The latter specifies relative width of the stability region of cylindrical morphology.

Because the corona in the crew-cut micelle is weakly curved,  $R_i \gg H_{i,\text{corona}} \approx H_{1,\text{corona}}$ , and  $F_{i,\text{core}}$  is typically noticeably smaller than  $F_{i,\text{corona}}$ , area  $s$  in eq 7 is specified with good accuracy by the balance condition  $F_{\text{surface}} \simeq F_{i,\text{corona}} \approx F_{1,\text{corona}}$  or, equivalently

$$\frac{\partial F_{1,\text{corona}}}{\partial s} = k_B T \gamma a^{-2} \quad (8)$$

By using eq 3 and taking into account that  $H_{1,\text{corona}} \simeq H_{1,\text{brush}}(s/n_A)$ , eq 7 can be presented at arbitrary  $n_A$  and  $n_B$  as

$$N_B^{(1-c),(c-s)}(n_A, n_B) = \frac{n_A^2}{n_B^2} N_B^{(1-c),(c-s)}(1, 1) \quad (9)$$

where binodals  $N_B^{(1-c),(c-s)}(1,1)$  for a linear diblock copolymer with  $n_A = n_B = 1$  depend only on the properties of block A and surface tension  $\gamma$ .

Therefore, irrespective of the nature of the coronal chains A (e.g., ionic or neutral) and environmental conditions (e.g., ionic strength and pH, solvent quality), an increase in the number  $n_B$  of insoluble core-forming blocks leads to the decrease in  $N_B^{(1-c)} \simeq N_B^{(c-s)} \sim n_B^{-2}$ . That is, an addition of solphophobic blocks to star-like macromolecule or redistribution of fixed number  $M_B$  of insoluble monomer units into a larger number  $n_B$  of insoluble

blocks can change the shape of the micelle from spherical to cylindrical (or to lamellar).

We focus first on a miktoarm star copolymer with nonionic soluble blocks A. The thickness and the free energy per chain of a planar brush of neutral chains A tethered with grafting area  $s/n_A$  are given, respectively, by

$$H_{1,\text{brush}} \approx aN_A(sa^{-2}/n_A)^{(\nu-1)/2\nu} \quad (10)$$

$$\frac{F_{1,\text{brush}}(s/n_A)}{k_B T} \approx N_A(sa^{-2}/n_A)^{-1/2\nu} \quad (11)$$

with  $\nu \approx 3/5$  and  $\nu = 1/2$  for good and theta solvent conditions, respectively.

Although soluble blocks A are chemically linked to a common junction localized at the core/corona interface (see Figure 2), the corresponding extra crowding is noticeable only at distances  $r \leq s^{1/2}$  from the interface, whereas at larger distances  $r \geq s^{1/2}$  the conformations of the A blocks are dictated by the core geometry. Therefore, the corona thickness  $H_{1,\text{corona}} \approx H_{1,\text{brush}}(s/n_A)$  and

$$F_{1,\text{corona}}/k_B T \approx n_A F_{1,\text{brush}}(s/n_A) = n_A N_A(sa^{-2}/n_A)^{-1/2\nu} \quad (12)$$

The equilibrium area  $s$  per star-like molecule is specified by eq 8 as

$$\frac{sa^{-2}}{n_A} \approx (N_A/\gamma)^{2\nu/(1+2\nu)} \quad (13)$$

By substituting  $H_{1,\text{corona}} = H_{1,\text{brush}}$ ,  $F_{1,\text{corona}}$ , and  $s$  from eqs 10, 12, and 13, and by omitting numerical coefficients, the binodal lines corresponding to cylinder-to-sphere (c-s) and lamella-to-cylinder (l-c) transitions are formulated as

$$N_B^{(l-c),(c-s)} \approx \frac{n_A^2}{n_B} N_A^{11\nu/(2+4\nu)} \gamma^{(2-7\nu)/(2+4\nu)} \quad (14)$$

An equivalent representation of binodals in  $M_A$ ,  $M_B$  coordinates is

$$\begin{aligned} M_B^{(l-c),(c-s)} &\approx \frac{n_A^{(4-3\nu)/(2+4\nu)}}{n_B} M_A^{11\nu/(2+4\nu)} \gamma^{(2-7\nu)/(2+4\nu)} \\ &= \frac{n_A^{(4-3\nu)/(2+4\nu)}}{n_B} M_B^{(l-c),(c-s)}(1, 1) \end{aligned} \quad (15)$$

where  $M_B^{(l-c)}(1,1)$  and  $M_B^{(c-s)}(1,1)$  are the binodals for the linear diblock copolymer with  $M_A = N_A$  and  $M_B = N_B$ .

Equations 14 and 15 permit us to analyze displacement of binodals due to branching of the macromolecule. In Figure 3 we demonstrate part of the theoretical phase diagram constructed for a dilute solution of a poly(styrene)-*block*-poly(isoprene) (PS-*b*-PI) block copolymer in selective solvent heptane.<sup>8</sup> The latter is close to theta solvent for PI ( $\nu = 1/2$ ) and is a poor solvent for PS. Binodals for the linear block copolymer  $M_B^{(l-c)}(1,1)$  and  $M_B^{(c-s)}(1,1)$  are shown by solid lines. A symmetric increase in the number of blocks  $n_B = n_A = 2$  accompanied by their concomitant shortening (that is, replacing the linear diblock copolymer by a 4-miktoarm star) leads to the shift in binodal lines to smaller values of  $M_B$  at fixed  $M_A$  (shown by dashed lines calculated according to eq 15).

Similarly to branching, intramolecular cyclization could also strongly affect the block copolymer self-assembly. In terms of

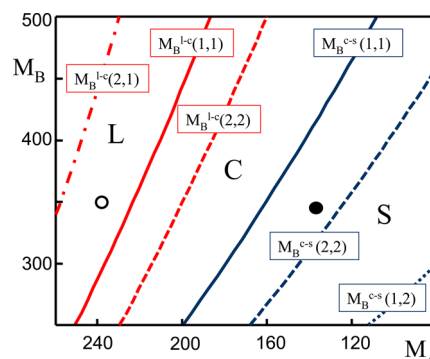


**Figure 3.** Diagram of states for copolymers with PS and PI blocks in heptane. Regions of thermodynamic stability of lamellae, cylinders, and spherical micelles are denoted as L, C, and S, respectively. The binodal lines separating stability regions of lamellae and cylindrical aggregates, (l-c), are marked in red, and those separating stability regions of cylinders and spheres, (c-s), are marked in blue. Binodals  $M_B^{(l-c)}(1,1)$  and  $M_B^{(c-s)}(1,1)$ , for linear diblock copolymer ( $n_A = n_B = 1$ ), are shown by solid lines. Dashed lines  $M_B^{(l-c)}(2,2)$  and  $M_B^{(c-s)}(2,2)$  indicate displacement of binodals due to the transformation of the linear block copolymer into a 4-miktoarm star (with  $n_A = n_B = 2$ ) or due to cyclization. Dotted blue line  $M_B^{(c-s)}(1,2)$  is the binodal for a block copolymer with cyclic core block B or 3-miktoarm star with  $n_A = 1$ ,  $n_B = 2$ . Red dash-dotted line  $M_B^{(l-c)}(2,1)$  is binodal for block copolymer with cyclic coronal block A or for a 3-miktoarm star with  $n_A = 2$ ,  $n_B = 1$ .

the scaling model, the association behavior of the miktoarm star-like copolymer with two soluble ( $n_A = 2$ ) and two insoluble ( $n_B = 2$ ) blocks with lengths  $N_A$  and  $N_B$  is equivalent to that of a cyclic block copolymer with respective lengths  $2N_A$  and  $2N_B$  of the blocks (see Figure 1b). This equivalence follows from the presumed strong stretching of the blocks in a micelle. Cross-linking of the free ends of stretched blocks leads to the corresponding entropy loss of about  $k_B T$  per chain, which is negligible compared to the total free energy of block copolymer  $F_i$  in the micelle. Therefore, binodals calculated for miktoarm stars can also be used to monitor the effect of block copolymer cyclization. As follows from the diagram in Figure 3, transformation of a linear block copolymer forming spherical micelles (i.e., with composition to the right of binodal line  $M_B^{(c-s)}(1,1)$ , marked by filled black circles in Figure 3) into a cyclic copolymer with the same length of the blocks (or, equivalently, to a miktoarm star with  $n_B = n_A = 2$ ) leads to destabilization of spherical morphology. That is, a filled black circle is found to the left of binodal  $M_B^{(c-s)}(2,2)$ , and association of the cyclic copolymer should give rise to cylindrical micelles. This is in agreement with the experimental observations.<sup>26–28</sup> According to refs 26–28, linear block copolymer PS<sub>290</sub>-*b*-PI<sub>110</sub> (subscript indicates the degree of polymerization of the corresponding block) self-assembled in heptane, giving rise to spherical micelles whose size and aggregation number were almost independent of solution concentration. Cyclization of the macromolecule leads, however, to formation of wormlike cylindrical micelles with concentration-dependent length. Although PS<sub>290</sub>-*b*-PI<sub>110</sub> is out of the stability range of spherical morphology in Figure 3 (possibly due to a different preparation protocol), its cyclization leads to a change in the aggregate shape from spherical to cylindrical, in agreement with prediction of the scaling model.

An even stronger effect is expected if cyclization involves only the insoluble block B of the linear diblock copolymer,<sup>29</sup>

which corresponds to a miktoarm star with  $n_A = 1$ ,  $n_B = 2$  (see Figure 1c). The position of binodal  $M_B^{(c-s)}(1,2)$  in this case is shifted further to the right and is shown in Figure 3 by a dotted line (calculated according to eq 15). When, however, the soluble block is made cyclic ( $n_A = 2$ ,  $n_B = 1$ ), binodals get shifted in the opposite direction indicating stabilization of nonplanar aggregate morphologies. For example, the linear block copolymer with composition marked by empty circle gives rise to cylindrical micelles in the solution after cyclization of coronal block A. The position of binodal  $M_B^{(l-c)}(2,1)$  calculated according to eq 15 is shown by a dash-dotted line in Figure 3. The presented formalism is applicable not only to nonionic copolymers but also to block copolymer with ionic (polyelectrolyte) soluble block. By substituting the corresponding expressions<sup>31</sup> for  $F_{1,corona}(s)$  and  $H_{1,corona}(s)$  for polyelectrolyte block A in eq 7, one could analyze the shift in binodals due to branching (cyclization) of copolymer with ionic soluble block.

In conclusion, we demonstrate that self-assembly of block copolymer in dilute solution is controlled not only by its composition  $M_A/M_B$  and solvent selectivity but also strongly depends on the architecture of the macromolecule. In particular, an increase in number  $n_B$  of insoluble arms (blocks) in the miktoarm star leads to destabilization of spherical morphology and promotes transition to cylindrical or lamellar-shaped aggregates. This trend holds even if the total number  $M_B$  of monomer units in insoluble blocks is kept constant. The relative shift in binodals due to increasing  $n_B$  is given by the universal power law dependence with the exponent independent of the nature of soluble blocks A. The same trend is predicted in the case of cyclization of insoluble block B in the diblock AB copolymer. In both cases, destabilization of spherical morphology is explained by increasing the entropic penalty for stretching a larger number of blocks B or cyclic block B in the micellar core. On the contrary, an increase in number  $n_A$  of soluble arms in the miktoarm star (or, similarly, cyclization of soluble block A in diblock copolymer) stabilizes the spherical geometry of self-assembled micelles. The shift in binodals due to an increase in number  $n_A$  of soluble blocks depends on the state (charged or neutral) of coronal blocks and environmental conditions (salinity, pH, solvent quality) in the solution.

## AUTHOR INFORMATION

### Corresponding Author

\*E-mail: oleg.borisov@univ-pau.fr.

### Notes

The authors declare no competing financial interest.

## ACKNOWLEDGMENTS

This work has been partially supported by the Russian Foundation for Basic Research (Grant 11-03-00969a) and by Department of Chemistry and Material Science of the Russian Academy of Sciences.

## REFERENCES

- (1) Riess, G. *Prog. Polym. Sci.* **2003**, *28*, 1107.
- (2) Quémener, D.; Deratani, A.; Lecommandoux, S. *Top. Curr. Chem.* **2012**, *322*, 165.
- (3) Borisov, O. V.; Zhulina, E. B.; Leermakers, F. A. M.; Müller, A. H. E. *Adv. Polym. Sci.* **2011**, *41*, 57.
- (4) Moughton, A. O.; Hillmyer, M. A.; Lodge, T. P. *Macromolecules* **2012**, *45*, 2.
- (5) Zhulina, E. B.; Borisov, O. V. *Macromolecules* **2012**, *45*, 4429.
- (6) Mai, Y.; Eisenberg, A. *Chem. Soc. Rev.* **2012**, *41*, 5969.
- (7) Zhulina, Y. B.; Birshtein, T. M. *Vysokomol. Soedin.* **1985**, *A27*, 511; *ibid.* **1987**, *A29*, 1524.
- (8) Zhulina, E. B.; Adam, M.; LaRue, I.; Sheiko, S. S.; Rubinstein, M. *Macromolecules* **2005**, *38*, 5330.
- (9) Borisov, O. V.; Zhulina, E. B. *Macromolecules* **2003**, *36*, 10029; *ibid.* **2005**, *38*, 6726; *Langmuir* **2005**, *21*, 3229.
- (10) Victorov, A. I.; Plotnikov, N. V.; Hong, P.-G. *J. Phys. Chem. B* **2010**, *114*, 8846.
- (11) Venev, S. V.; Reineker, P.; Potemkin, I. I. *Macromolecules* **2010**, *43*, 10735.
- (12) Milner, S. T. *Macromolecules* **1994**, *27*, 2333.
- (13) Junnila, S.; Houbenov, N.; Karatsas, A.; Hadjichristidis, N.; Hirao, A.; Iatrou, H.; Ikkala, O. *Macromolecules* **2012**, *45*, 2850.
- (14) Beyer, F. L.; Gido, S. P.; Uhrig, D.; Mays, J. W.; Tan, N. B.; Trevino, S. F. *J. Polym. Sci., Part B: Polym. Phys.* **1999**, *37*, 3392.
- (15) Fludas, G.; Pispas, S.; Hadjichristidis, N.; Pakula, T.; Erukhimovich, I. *Macromolecules* **1996**, *29*, 4142.
- (16) Pispas, S.; Hadjichristidis, N.; Mays, J. W. *Macromolecules* **1996**, *29*, 7378.
- (17) Pispas, S.; Hadjichristidis, N.; Potemkin, I.; Khokhlov, A. *Macromolecules* **2000**, *33*, 1741.
- (18) Hinestroza, J. P.; Uhrig, D.; Pickel, D. L.; Mays, J. W.; Kilbey, S. M., II *Soft Matter* **2012**, *8*, 10061.
- (19) Hinestroza, J. P.; Alonso, J.; Osa, M.; Kilbey, S. M., II *Macromolecules* **2010**, *43*, 7294.
- (20) Ramzi, A. Q.; Prager, M.; Richter, D.; Efstratiadis, V.; Hadjichristidis, N.; Young, R. N.; Allgaier, J. B. *Macromolecules* **1997**, *30*, 7171.
- (21) Wang, X. S.; Winnik, M. A.; Manners, I. *Macromol. Rapid Commun.* **2003**, *24*, 403.
- (22) Gorodyska, G.; Kiriya, A.; Minko, S.; Tsitsilianis, C.; Stamm, M. *Nano Lett.* **2003**, *3*, 365.
- (23) Erdogan, T.; Ozyurek, Z.; Hizai, G.; Tunca, U. *J. Polym. Sci., Part A: Polym. Chem.* **2004**, *42*, 2313.
- (24) Gao, H.; Matyjaszewski, K. *J. Am. Chem. Soc.* **2007**, *129*, 11828.
- (25) Plamper, F. A.; McKee, A.; Laukanen, A.; Nykänen, A.; Walther, A.; Aseyev, V.; Rukolainen, J.; Tenhu, H. *Soft Matter* **2009**, *5*, 1812.
- (26) Borsali, R.; Minatti, E.; Putaux, J.-L.; Schappacher, M.; Deffieux, A.; Viville, P.; Lazzaroni, R.; Narayanan, T. *Langmuir* **2003**, *19*, 6.
- (27) Putaux, J.-L.; Minatti, E.; Lefebvre, C.; Borsali, R.; Schappacher, M.; Deffieux, A. *Faraday Discuss.* **2005**, *128*, 1.
- (28) Minatti, E.; Viville, P.; Borsali, R.; Schappacher, M.; Deffieux, A.; Lazzaroni, R. *Macromolecules* **2003**, *36*, 4125.
- (29) Londale, D. E.; Monteiro, M. J. *J. Polym. Sci., Part A: Polym. Chem.* **2011**, *49*, 4603.
- (30) Semenov, A. N. *Sov. Phys. JETP* **1985**, *61*, 733.
- (31) Zhulina, E. B.; Birshtein, T. M.; Borisov, O. V. *Eur. Phys. J. E* **2006**, *20*, 243.